

NEAR-INFRARED IMAGES OF MG 1131+0456 WITH THE W. M. KECK TELESCOPE: ANOTHER DUSTY GRAVITATIONAL LENS?¹

J. E. LARKIN,² K. MATTHEWS,² C. R. LAWRENCE,² J. R. GRAHAM,^{2,3,4} W. HARRISON,⁵ G. JERNIGAN,⁶ S. LIN,²
 J. NELSON,³ G. NEUGEBAUER,² G. SMITH,⁵ B. T. SOIFER,² AND C. ZIOMKOWSKI²

Received 1993 July 13; accepted 1993 October 12

ABSTRACT

Images of the gravitational lens system MG 1131+0456 taken with the near-infrared camera on the W. M. Keck telescope in the *J* and *K_s* bands show that the infrared counterparts of the compact radio structure are exceedingly red, with $J-K > 4.2$ mag. The *J* image reveals only the lensing galaxy, while the *K_s* image shows both the lens and the infrared counterparts of the compact radio components. After subtracting the lensing galaxy from the *K_s* image, the position and orientation of the compact components agree with their radio counterparts. The broad-band spectrum and observed brightness of the lens suggest a giant galaxy at a redshift of ~ 0.75 , while the color of the quasar images suggests significant extinction by dust in the lens. There is a significant excess of faint objects within $20''$ of MG 1131+0456. Depending on their mass and redshifts, these objects could complicate the lensing potential considerably.

Subject headings: dust, extinction — galaxies: interactions — gravitational lensing — quasars: individual (MG 1131+0456)

1. INTRODUCTION

MG 1131+0456 was the first gravitational lens system observed in which the extended lobe of a distant radio source was imaged into a complete ring by an intervening galaxy (Hewitt et al. 1988; Kochanek et al. 1989). Two compact radio components are also observed with a separation of $2''.045$ at 22 GHz (Chen & Hewitt 1993). Hewitt et al. (1988) obtained an image in the *R* band showing a faint 22 mag extended object at the position of the radio source, but no sign of optical counterparts to the compact radio components. Hammer et al. (1991) made long exposures through *B*, *V*, *R*, and *i* filters. Following subtraction of standard galaxy models from the sum of their *R* and *i* images, they found a ringlike residual similar to the radio ring, which they interpreted as the lensed image of the optical emission from the radio source.

In the model of Kochanek et al. (1989), the radio source consists of two extended lobes extending continuously from a relatively bright core. Objects with similar radio structures in the MIT-Green Bank survey are typically identified with galaxies, although some are identified with quasars (Lawrence et al. 1984, 1986). The MG sources are sometimes very faint optically, so the lack of any compact optical counterparts to the images of the radio core was not terribly surprising by itself. At $2.2 \mu\text{m}$ (*K* band), however, both extended emission and prominent compact components are seen, although the separation disagrees with that of the radio components (Annis 1992). If the compact components are multiple images of a nuclear optical component, their absence at optical frequencies requires explanation. To understand the relationship between the *K* image

and the optical and radio images, we observed MG 1131+0456 at both 1.27 and $2.15 \mu\text{m}$ with the near-infrared camera (NIRC) on the Keck telescope.

2. OBSERVATIONS AND DATA REDUCTION

MG 1131+0456 was observed on 1993 March 22 and 23 using the NIRC on the 10 m W. M. Keck telescope on Mauna Kea. The camera uses a 256×256 element InSb array with a scale size of $0''.15 \text{ pixel}^{-1}$, giving a total field of $38''.4 \times 38''.4$. A detailed description of the camera is given by Matthews (1993). Thirteen images were obtained in the *K_s* (*K*-short) band, which covers $1.99\text{--}2.32 \mu\text{m}$ and 24 images were obtained in the *J* band, which covers $1.11\text{--}1.40 \mu\text{m}$. The integration time was 21 s for all images, giving total integration times of 504 s in the *J* band and 273 s in the *K_s* band. To allow an accurate determination of the gain and sky background on each pixel, the object was placed at many different positions on the array.

Sky frames for each band were constructed by finding the median value at each pixel in the array of all the images in that band. No residual images of stars can be seen in these frames. After the sky background was subtracted from each image, pixel-to-pixel gain variations were corrected by dividing each image by a normalized version of the sky frame.

The individual images were aligned using two bright stars in the field. Bilinear interpolation was used for fractional pixel shifts. We estimate uncertainties in these shifts of ~ 0.3 pixels or $0''.05$, based on variations in the centroid position of the brightest star in the field between frames taken at the same guider position. The images were shifted to their correct positions and mosaiced by taking the median of the overlapping frames at each pixel. The $\sim 0''.8$ FWHM of the stars in both bands did not change due to the mosaicing process. Magnitude calibration was based on images of the UKIRT faint standard star M13-A14.

The final mosaics are shown in Figure 1 (Plate L6). The *K_s* image shows the same structure as the *K* image of Annis (1992). The *J* image is dramatically different from the *K_s* image, but is similar to the *R* images of Annis (1992) and Hammer et al. (1991).

¹ Based on observations obtained at the W. M. Keck Observatory, which is operated jointly by the California Institute of Technology and the University of California.

² Palomar Observatory, California Institute of Technology, 320-47, Pasadena, CA 91125.

³ Astronomy Department, University of California, Campbell Hall, Berkeley, CA 94720.

⁴ Alfred P. Sloan Research Fellow.

⁵ California Association for Research in Astronomy, Kamuela, HI 96743.

⁶ Space Science Laboratory, University of California, Berkeley, CA 94720.

PLATE L6

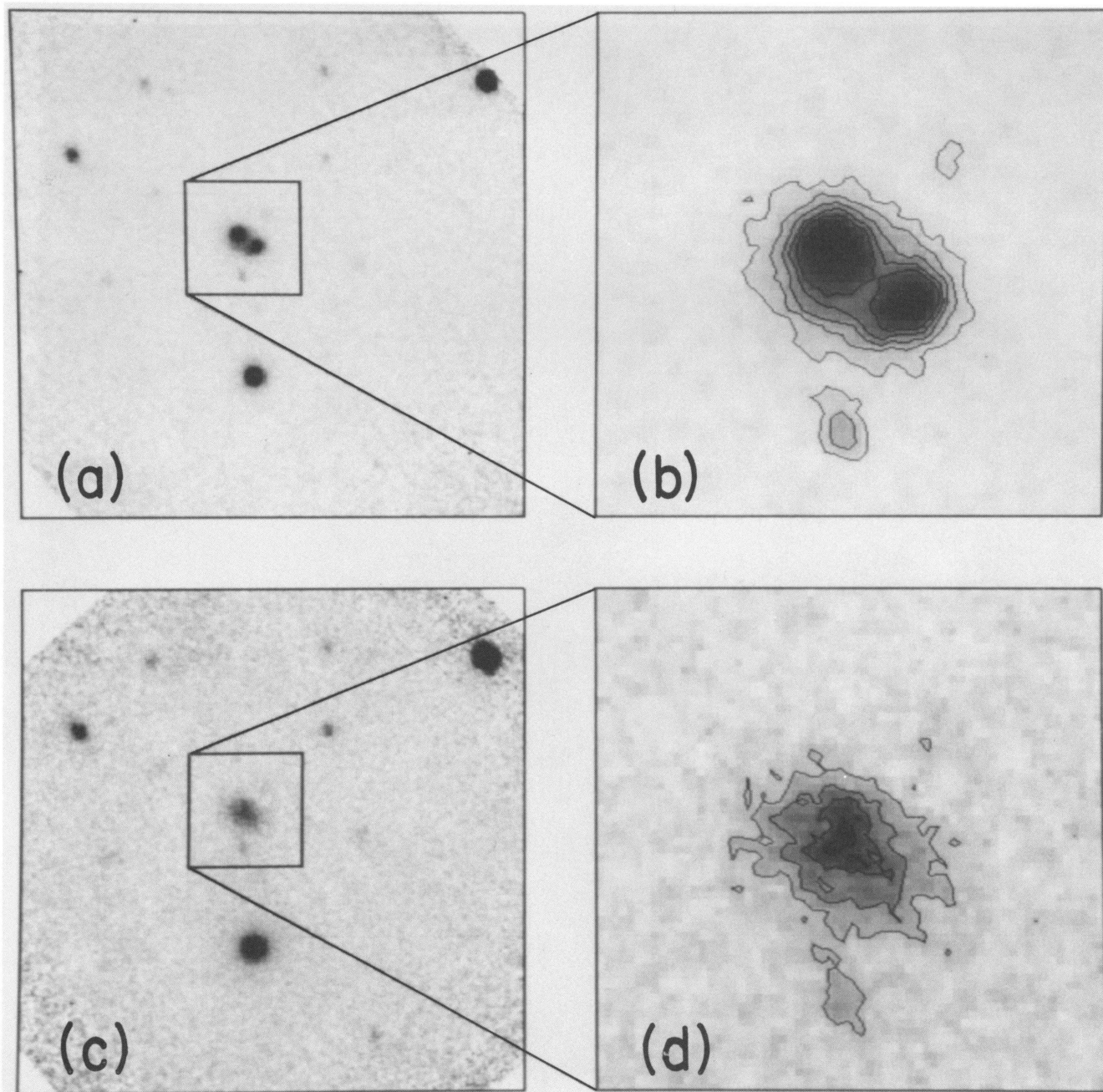


FIG. 1.—(a)–(b) K_s image of MG 1131 + 0456, rotated so that north is at the top, east is to the left. The total exposure time of 273 s was obtained in 13 exposures of 21 s. The full image is 280×280 pixels ($42''.0 \times 42''.0$); the detail region is 64×64 pixels ($9''.6 \times 9''.6$). (c)–(d) J image. The total exposure time of 504 s was obtained in 24 exposures of 21 s. Image sizes are the same as K_s .

LARKIN et al. (see 420, L9)

3. ANALYSIS

The J image in Figure 1c and 1d shows only diffuse emission, while the K_s image shows both diffuse and compact emission. A combination of diffuse and compact emission is hardly surprising in gravitational lens systems, but the dramatic difference between the J and K_s images, and their correspondence with radio images, must be explained. Following Hewitt et al. (1988), we call the northeastern compact component A, and the other B.

The final J and K_s images can be aligned with each other using stars in the field, with an uncertainty of no more than $0''.03$. It is more difficult to align the infrared and radio images, because there are no isolated, unresolved objects detected at both radio and infrared frequencies. It is tempting to identify the compact components in the K_s image, separated by $1''.84$ (in agreement with Annis 1992), as the infrared counterparts of the compact radio components. However, the fact that this separation is significantly less than the $2''.15$ separation of the peaks in the 15 GHz image of Hewitt et al. (1988) must be explained.

To establish the true separation of the lensed images of the compact core in the K_s image, the galaxy must be subtracted. A profile through the positions of A and B in the J image shows no sign of any unresolved emission near those positions. There is also no reason to expect significant infrared emission from the steep spectrum radio lobe which is imaged into the radio ring. We make the initial assumption, therefore, that the emission seen in the J image is entirely from the lensing galaxy.

The J image was scaled and subtracted from the K_s image. The scale factor was chosen by trial and error to give the smoothest residuals, evaluated by eye, in the important region between A and B dominated by the galaxy. Although this is somewhat subjective, the irregularity of the emission from the galaxy, the likelihood that the color of the galaxy is not uniform, and the proximity of two field objects makes a simple calculation of the rms residual inappropriate. Figure 2a (Plate L7) shows the difference image. A point-spread function (PSF) determined from stars in the K_s frame was then fitted to the two compact components shown in Figure 2a. Table 1 gives relative positions and photometry for the galaxy and compact components. Figure 2b shows the residual flux which

could not be assigned to either the lensed images or to the initial approximation of the lensing galaxy. The residual flux is diffuse and constitutes only $\sim 10\%$ of the K -band flux of the system. We interpret it as the difference between the galaxy at J and K_s and add it to the scaled J image to obtain the K_s galaxy model shown in Figure 2c (for comparison, Figure 1d is the galaxy at J).

The compact radio core separation of $2''.045$ found by Chen & Hewitt (1993) in a $0''.08$ resolution 22 GHz map is in excellent agreement with the $2''.01$ separation of the two compact sources observed in the K_s image after galaxy subtraction. The position angles determined in the radio and the infrared also agree to within $1''.5$. This agreement justifies the identification of the K -band peaks with the images of the radio core. Based on this association, the infrared and radio images can be aligned accurately. The uncertainty in this alignment is basically the $0''.05$ uncertainty in the centroid of the PSF fits. With this alignment, we place an upper flux limit of 22 mag for point sources at positions A and B in the J image.

The lumpiness of the galaxy makes its "position" somewhat indeterminate. Centroids depend on the aperture size, are different in the two bands, and are offset from the emission peak for even modest apertures (see footnotes to Table 1). Nevertheless, by any measure the center of the galaxy is between the quasar images as expected. Kochanek et al. (1989) argued that the major axis of an elliptical potential must be perpendicular to the major axis of the ring, despite suggestions to the contrary from the R image of Hewitt et al. (1988). Contours plotted on the total J emission (see Fig. 1d) show that the major axis of the inner isophotes is almost perpendicular to the major axis of the outer isophotes. The infrared images thus suggest an explanation for this apparent contradiction and justify the use of a more complicated potential in lens models. We see no evidence for the ringlike residual found by Hammer et al. (1991) in their $R + i$ image, and we think it much more likely that the ring represents a combination of intrinsic structure and systematic color differences in the lensing galaxy.

In addition to the present J and K_s measurements, MG 1131+0456 has been observed at B (>25 mag), V (22.66 ± 0.25 mag), R (22.14 ± 0.07 mag), and i (20.67 ± 0.08 mag) by Hammer et al. (1991). Since we believe that in all

TABLE 1
ASTROMETRY AND PHOTOMETRY

COMPONENT	RADIO ^a			INFRARED ^b			J (mag)	K (mag)
	$\Delta\alpha$	$\Delta\delta$	$\left(\frac{S}{S_B}\right)$	$\Delta\alpha$	$\Delta\delta$	$\left(\frac{S}{S_B}\right)$		
A	1''.73	1''.09	0.72	1''.68	1''.11	0.91	>22	17.9 ± 0.1
B	0.00	0.00	1.00	0.00	0.00	1.00	>22	17.8 ± 0.1
C	-0.44	-0.50	<0.3
Lens	1.27 ^c	0.81 ^c	...	d	d	2.75	18.7 ± 0.1	16.8 ± 0.2

^a At 22 GHz, from Chen & Hewitt 1993. Radio position uncertainties are less than $0''.01$. Flux density ratios are relative to source B.

^b Lens from J image, scaled for best fit. Two unresolved components (i.e., PSF from star) fitted at peaks. Magnitudes have been corrected from the observed K_s band to the more normal K band. Flux density ratios are for the K_s band relative to source B. Infrared position uncertainties are less than $0''.1$.

^c Lens position from model of Kochanek et al. 1989, referenced to the position of B in the 22 GHz image of Chen & Hewitt 1993.

^d The structure of the galaxy is complex, and its position cannot be represented by a single pair of numbers. For example, the centroids of the entire galaxy in J and K_s are offset from B by $(1''.32, 0''.44)$ and $(1''.22, 0''.5)$, respectively. The peaks in J and K_s are offset from B by $(1''.28, 0''.84)$ and $(1''.35, 1''.07)$, respectively. And the centroids in a $0''.6$ radius around the peaks in J and K_s are offset by $(1''.29, 0''.66)$ and $(1''.37, 0''.93)$, respectively.

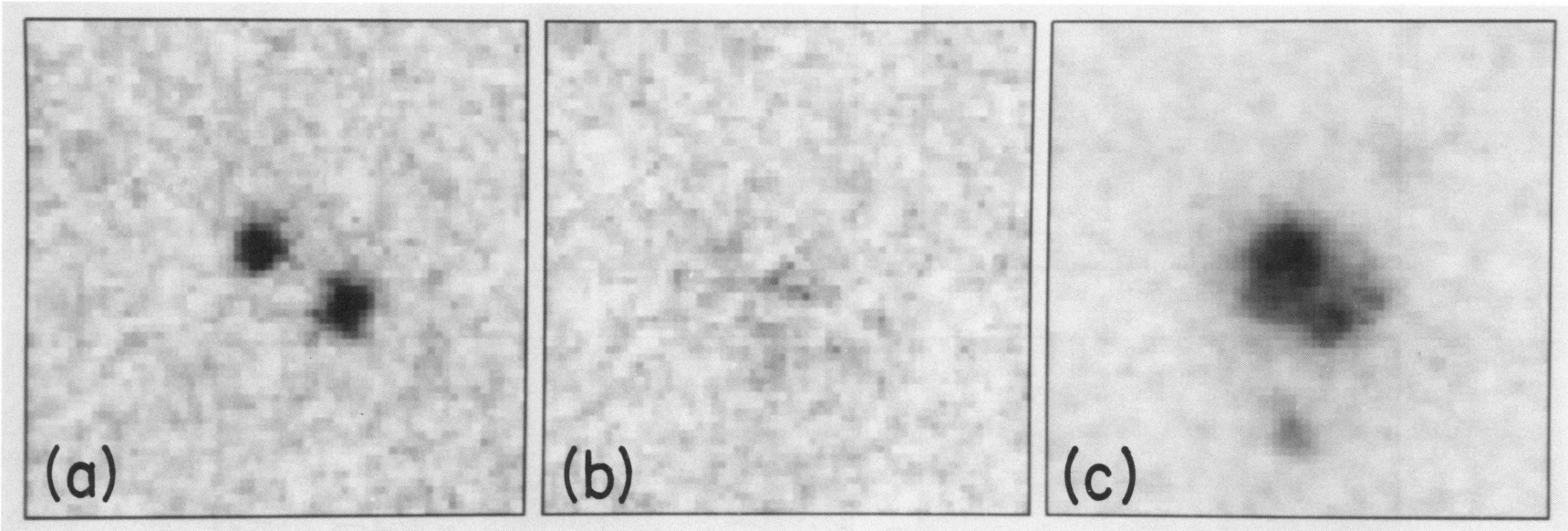


FIG. 2.—(a) K_s image after subtraction of the J image scaled to leave the smoothest residuals in the region between A and B. (b) The same, following subtraction of best-fitting PSFs derived from a nearby star. The residual flux is less than 10% of the diffuse flux in the original image. (c) The sum of the scaled J image and the residual in the previous panel, that is, the lensing galaxy at K_s band without the compact components. Each field is 64×64 pixels ($9''.6 \times 9''.6$).

LARKIN et al. (see 420, L10)

bands blueward of K only the lensing galaxy itself is seen, we treat the measurements of Hammer et al. as being of the lens itself. Comparing these measurements with the redshifted spectrum of the nearby elliptical galaxy NGC 4889 in Coma, we find reasonable agreement at $z = 0.91$, although at that redshift NGC 4889 would be 10% and 20% brighter in J and K , respectively, and 40% dimmer in V than the lensing galaxy. Without the V measurement, which has the largest uncertainty, the K_s , J , i , and R magnitudes agree very well with those of NGC 4889 for redshifts in the range 0.7–0.9, with the best agreement at $z = 0.75$. To the extent that broad-band photometry justifies any redshift estimate, we conclude that the galaxy in MG 1131+0456 very likely has a spectrum much like nearby giant ellipticals at a redshift of ~ 0.8 . This value is consistent with $z = 0.85$ as found by Hammer et al. based on their optical spectrum.

The luminosity of the lens in MG 1131+0456 is consistent with it being somewhat fainter than brightest cluster galaxies or 3C radio galaxies. At $z = 0.75$, NGC 4889 would be 0.6 mag brighter in J than the lens in MG 1131+0456. At redshifts around 1, 3C radio galaxies typically have K magnitudes of about 17 (Rigler et al. 1992), and unevolving stellar synthesis models (Charlot & Bruzual 1991) for $M_{\text{tot}} = 1.5 \times 10^{12} M_{\odot}$ predict $K \approx 15.8$ mag ($H_0 = 75$, $q_0 = 0$, throughout).

An estimate of the quasar's redshift can be found from the model of Kochanek et al. (1989). Using $L \propto \sigma^4$ (e.g., Dressler 1987) for comparison to NGC 4889, and making a correction for passive stellar evolution (P. McCarthy 1993, private communication), we find a one-dimensional velocity dispersion σ for the lens in the neighborhood of 300 km s^{-1} . This implies that $1.7 < z_{\text{quasar}} < 3.5$. If the lens is dimmed somewhat by dust (see below), its inferred mass would increase, and the redshift of the quasar would decrease. Measured redshifts for both lens and quasar are obviously essential, but our main conclusions are insensitive to the redshifts.

Examination of the image shown in Figure 1 reveals 22 faint objects above the 3.5σ detection limit in a $38''$ square centered on the lens. Number counts of faint objects in other fields imaged during this run are consistent with those found in the deep K -band survey by Cowie et al. (1993). Those fields can therefore be used as control fields to determine the statistical significance of the faint objects near MG 1131+0456. Such an analysis shows that the MG 1131+0456 field has a 5σ excess of objects with $19 < K < 20$ mag. This excess does not include the two close "companions" to the lens (see Annis 1992), which also have K magnitudes in this range. If these objects lie between the radio source in MG 1131+0456 and us, and contain a significant amount of matter, they may seriously complicate the lensing potential.

4. DISCUSSION

The new infrared images of MG 1131+0456 demonstrate conclusively that the compact components seen in the K band are the counterparts of the lensed radio source and give the clearest view yet of the lensing galaxy.

The extreme color of the lensed object, $J - K > 4.2$ mag, however, is quite unusual. The reddest quasars found in radio samples are blazars, which have optical spectra dominated by a red Doppler-boosted synchrotron component (Impey, Lawrence, & Tapia 1991). Even for a spectral index of -2.6 , the steepest found in the highly polarized objects in Impey et al., $J - K = 2.6$ mag. While strong emission lines can have a sig-

nificant effect on color, the strongest lines observed in quasars, with rest equivalent width $\sim 700 \text{ \AA}$, would increase $J - K$ by only 0.75 mag. Since objects with such strong lines do not have red continua, they would still have $J - K$ much smaller than 4.2 mag.

It is always possible, of course, that MG 1131+0456 is the first of a new class of extremely red objects; however, appeals to uniqueness should be made only as a last resort. In gravitational lens systems, especially those where the images are seen through the lens, significant reddening by dust in the lens provides a natural explanation that must be considered first. Dust appears to play an important role in MG 0414+0534 (Lawrence et al. 1993), another lens system from the MG survey. We think it likely that dust is important in MG 1131+0456 as well.

Crude estimates of the amount of dust required to produce the observed colors of the lensed images in MG 1131+0456 can be made. Most quasars (most AGNs, in fact), with or without strong emission lines, have colors intermediate between the extremes represented by powder laws (v^α) with $-2.6 \leq \alpha \leq 0$. For such spectra, and for dust in the lens at a redshift between 0.7 and 1.0, visual extinction between 3.3 and 7.7 mag is required to produce $J - K \geq 4.2$ mag as observed. [We use extinction from Cardelli, Clayton, & Mathis 1989 for $\lambda > 5495 \text{ \AA}$, and the SMC extinction law from Prevot et al. 1984 for $\lambda < 5495 \text{ \AA}$, with $A_V/E(B - V) = 3.1$.] For lens redshifts less than 0.7 the required extinction increases rapidly, while at redshifts larger than 1 it decreases slowly. For example, at $z_{\text{lens}} = 1$, 3.3 mag of visual extinction would be required for $\alpha = -2.6$, while at $z_{\text{lens}} = 2$, 2.5 mag would still be required.

Three objections might be raised to so much dust in the lensing galaxy. First, the A/B flux ratio is different in the radio and the infrared by only 20%. If the dust is at $z = 0.75$, $A_V > 3.8$ mag is required even if the background quasar is intrinsically as red as the reddest object in the Pearson-Readhead sample. However, the *differential* reddening of 20% along the two paths through the lens separated by $\gtrsim 10$ kpc at $1.23 \mu\text{m}$ (corresponding to the observed K_s band) is equivalent to a difference in A_V of only 0.7 mag. That so much dust could be distributed so uniformly over so large an area, or alternatively just happen to be so similar along two paths not equidistant from the core of the galaxy, seems somewhat remarkable, especially considering the fact the image furthest from the nucleus (source B) is the one that is affected the most.

The second objection to dust in the lens is the good agreement between the broad-band colors of the lens and those of the giant elliptical galaxy NGC 4889 at $z = 0.75$. If dust is confined to an almost opaque disk, light from stars in front of the disk will be unaffected, while light from stars behind the disk would be so faint that its color would hardly matter. As long as enough stars are in front of the disk, the net effect of the dust is to dim the galaxy without changing its spectrum. Dust thoroughly mixed with stars has a larger effect. For $A_V = 3.5$ mag at $z = 0.55$, $E(B - K) = 1.73$ mag, $E(V - K) = 1.46$ mag, $E(R - K) = 1.19$ mag, $E(i - K) = 1.01$ mag, and $E(J - K) = 0.47$ mag. These color changes would make a dusty galaxy at $z = 0.55$ look much like a galaxy *without* dust at $z = 0.75$. A more realistic calculation that included the effects of scattering would give even smaller color differences (R. Elston 1993, private communication). This illustrates that significant amounts of dust can have a surprisingly small effect on the colors of a galaxy.

The third objection to dust in the lens is that the mass required in the lens to form the images we observe is large, comparable to that of giant elliptical galaxies rather than disk galaxies. At low redshift, at least, elliptical galaxies rarely have much dust; however, Centaurus A, often suggested to be an interacting galaxy, has a broad dust lane extending across the entire galaxy with relatively uniform visual extinction between 3.1 and 6 mag (Harding, Jones, & Rodgers 1981). Perhaps the lens in MG 1131+0456 is an interacting galaxy as well, with the dust supplied by a smaller merging disk system. Another (not unrelated) possibility is that elliptical galaxies had much more dust in the past. The blotchy appearance of the lensing galaxy is not inconsistent with either possibility, and the presence of two "companions" with very small ($\sim 3''$) projected distances supports the possibility of a past merger.

The intrinsic colors of radio-selected quasars are known at all redshifts, and no objects with similar colors have been found. Objects in the MG survey itself have not been completely identified, and the unmagnified background source in MG 1131+0456 is very weak compared to the sources in 5 GHz samples that have been completely identified. Work on fainter radio samples may well contain surprises.

On balance, it seems to us that the arguments against dust in the lens are weaker than the argument against an intrinsically red color for the lensed object. The fact that one of the ~ 13 well-established, radio-selected lens systems, MG 0414+0534, is already identified as a dusty lens (Lawrence et al. 1993)

makes the possibility that MG 1131+0456 is the second such dusty lens system seem much more plausible. The possibility that dust has a major impact on the observed properties of two of the ~ 13 well-established, radio-selected lens systems is significant. MG 0414+0534 and MG 1131+0456 could not have been found in any optical lens searches completed to date. It may well be that most radio lens systems with small separations and extremely faint, hard-to-classify optical counterparts will turn out to have dusty lenses at high redshift that significantly redden the quasar counterparts.

The W. M. Keck Observatory is operated as a scientific partnership between the California Institute of Technology and the University of California. It was made possible by the generous gift of the W. M. Keck Foundation, and the support of its president, Howard Keck. We are most grateful for their visionary endowment that has made possible the first of the next generation of telescopes. It is a pleasure to also thank E. Stone, W. Frazier, W. Sargent, S. Faber and all of the many devoted people whose unflagging efforts have made possible the success of the W. M. Keck Observatory. We thank Jeremy Mould for useful discussions, Pat McCarthy for useful discussions and the results of stellar synthesis models, and an anonymous referee for helpful suggestions. Infrared and radio astronomy at Caltech are supported in part by grants from the NSF and NASA.

REFERENCES

- Annis, J. 1992, *ApJ*, 391, L17
 Cardelli, J. A., Clayton, G. C., & Mathis, J. S. 1989, *ApJ*, 345, 245
 Charlot, S., & Bruzual, G. A. 1991, *ApJ*, 367, 126
 Chen, G. H., & Hewitt, J. N. 1993, *AJ*, submitted
 Cowie, L. L., Gardner, J. P., Hu, E. M., Wainscoat, R. J., & Hodapp, K. W. 1993, *ApJ*, submitted
 Dressler, A., Lynden-Bell, D., Burstein, D., Davies, R. L., Faber, S. M., Terlevich, R. J., & Wegner, G. 1987, *ApJ*, 313, 42
 Hammer, F., Le Fèvre, O., Angonin, M. C., Meylan, G., Smette, A., Surdej, J. 1991, *A&A*, 250, L5
 Harding, P., Jones, T. J., & Rodgers, A. W. 1981, *ApJ*, 251, 530
 Hewitt, J. N., Turner, E. L., Schneider, D. P., Burke, B. F., Langston, G. I., & Lawrence, C. R. 1988, *Nature*, 333, 537
 Impey, C. D., Lawrence, C. R., & Tapia, S. 1991, *ApJ*, 375, 46
 Kochanek, C. S., Narayan, R., Lawrence, C. R., & Blandford, R. D. 1989, *MNRAS*, 238, 43
 Lawrence, C. R., Bennett, C. L., Hewitt, J. N., & Burke, B. F. 1984, *ApJ*, 278, L95
 Lawrence, C. R., Bennett, C. L., Hewitt, J. N., Langston, G. I., Klotz, S. E., Burke, B. F., & Turner, K. C. 1986, *ApJS*, 61, 105
 Lawrence, C. R., Elston, R., Jannuzi, B. T., Turner, E. L., & Huang, X. 1993, *AJ*, in preparation
 Matthews, K. 1993, in preparation
 Prévot, M. L., Lequeux, J., Maurice, E., Prévot, L., & Rocca-Volmerange, B. 1984, *A&A*, 132, 389
 Rigler, M. A., Lilly, S. J., Stockton, A., Hammer, F., & Le Fèvre, O. 1992, *ApJ*, 385, 61